EBSD characterization of incoherent CSL grain boundaries in pure aluminum processed by severe plastic deformation

Yu, Y.D.[1], Liu, M.P.[2], Hjelen, J.[1] and Roven, H.J.[1]

[1] Department of Materials Science and Engineering, Norwegian University of Science and Technology, NO-7491 Trondheim, Norway, [2] School of Materials Science and Engineering, Jiangsu University, 212013 Zhenjiang, China

Grain boundary engineering (GBE) was first proposed by Watanabe [1] with the idea of GB design and control to achieve high performance structural materials. In recent years, nano-twinned materials with Σ3 coincidence site lattice (CSL) GBs, or twinned boundaries, have attracted great interest [2]. Low stacking fault energy (SFE) polycrystalline materials modified with high fractions of "special boundaries" (low CSL GBs), e.g. created by plastic deformation followed by annealing, have shown high resistances to fracture and corrosion, but also good mechanical properties including ductility. However, for pure aluminum with very high SFE, Σ3 boundaries inside Al grains have rarely been found except under certain extreme ultrahigh deformation conditions. In this work, the roles of CSL GBs in pure aluminum processed by severe plastic deformation were investigated by electron backscatter diffraction (EBSD).
Commercial pure aluminum samples were subjected to high pressure torsion (HPT) to ten turns with a rotation speed of 1 rpm under a pressure of 6 GPa at room temperature. Offline EBSD characterizations were carried out on a Zeiss Ultra FEG SEM by using the NORDIF3.0 EBSD and EDAX orientation imaging microscopy (OIM) systems. Cross sections of the post HPT longitudinal cylindrical sample were analyzed. EBSD investigations were performed both in the center and at the edge of the cross section and showed quite similar microstructure characteristics with homogeneous ultrafine equiaxed grains around one micrometer in size, i.e. see the representative inverse pole figure (IPF) map in Fig. 1. Also, high resolution EBSD scans with 50nm step-size were carried out in a small subarea as shown in Fig.2. Here, line-scan misorientations were followed along numerous lines and the line profiles were drawn as much as possible, perpendicular to the different GBs. The GBs appeared mostly as special boundaries and had various typical misorientation angles. Fig.3 shows one of the representative misorientation profiles which was measured along the black line in Fig.2. Here no obvious misorientation gradients could be observed inside grains. These special boundaries were further analyzed and classified by using the Brandon Criterion [3] as shown in Fig.4. They appeared as different CSL GBs, and Σ3 boundaries were colored as red lines, Σ9 and Σ27(a) as blue and yellow lines, respectively. The partial curved nature of these boundaries indicated that they were incoherent CSL GBs. The Σ9 and Σ27(a) special boundaries were quite possible due to the reaction product of different Σ3 GBs. In a previous work [4] on high SFE Al investigated by TEM, no Σ3 twinned boundaries were observed. The essential defect-structure contained a small-scale feature involving two partial dislocations connected by a stacking fault having a length around 5nm. Similar observations could of course not be detected under the EBSD resolution conditions giving the map shown in Fig.2. During the HPT process the microstructure was transformed to ultrafine grains, which is also reflected in the present line scan misorientation map shown in Fig.3. The lack of misorientation gradients inside the grains indicated low dislocation densities. From these results one may assume that the dislocation movements occurring during HPT act as a driving force for creating the energy favorable incoherent CSL GBs, i.e. generated with a relative lower energy than for normal random high angle GBs.

[1] Watanabe T., Res. Mechanica 11, 47 (1984).

[2] Lu K., Lu L. and Suresh S., Science 324(5925), 349 (2009).

[3] Brandon D.G., Acta Metall. 14, 1479(1966).

[4] Yu Y.D., Liu M.P., Hjelen J and Roven H.J., IMC18(2014).

Fig.1 IPF map of the cross-section overview.

Fig.2 High resolution IPF map with 50nm scan step.

Fig.3 The misorientation line profile along the black line shown in Fig.2.

Fig.4 Image quality (IQ) map of Fig.2 overlapped with Σ3(red), Σ9(blue) and Σ27(yellow) GBs.

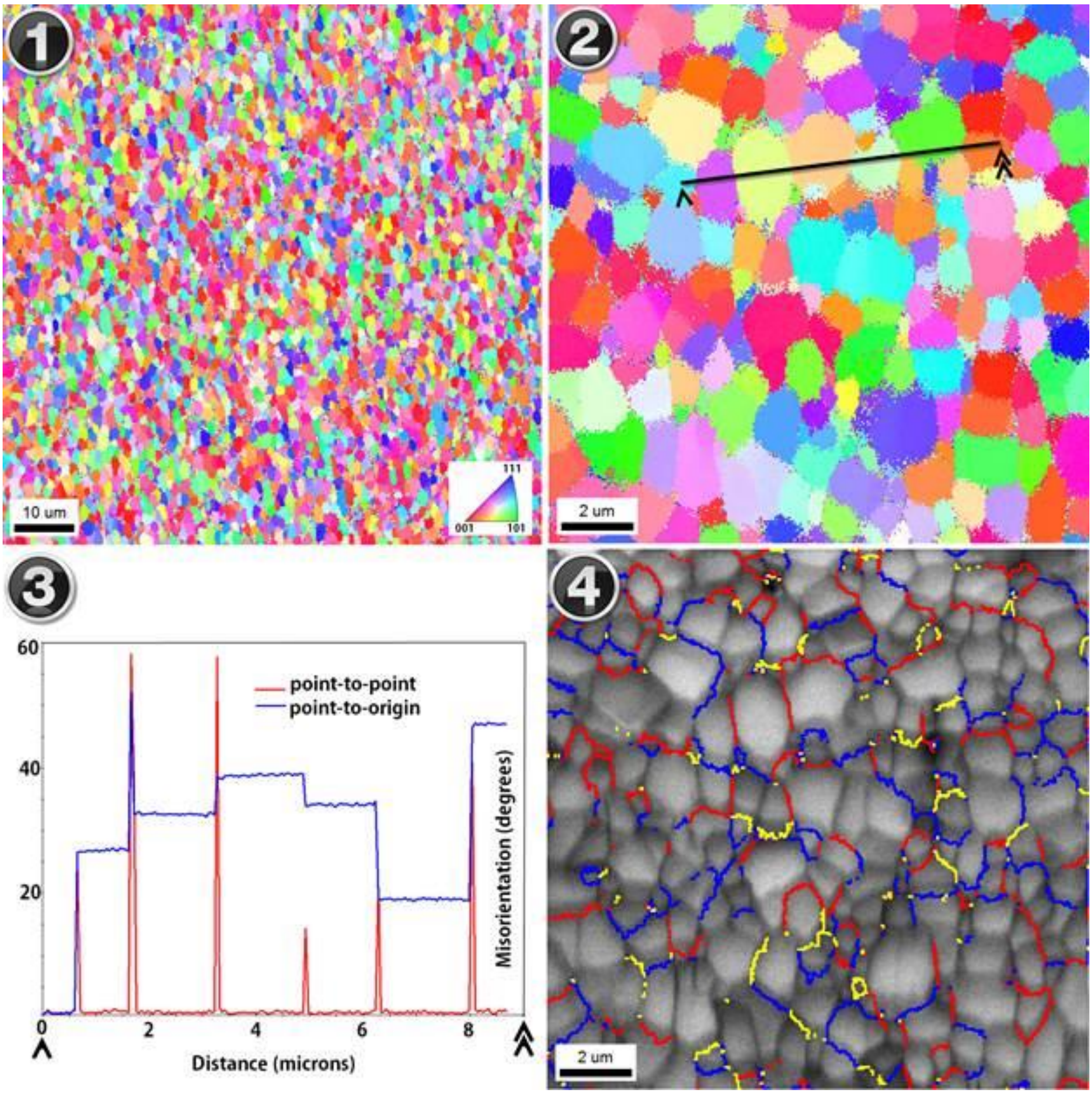

1
10 um
111
001
101
2
2 um
3
60
40
20
0
2
4
6
8
point-to-point
point-to-origin
Misorientation (degrees)
Distance (microns)
4
2 um